IEEE Access
Multidisciplinary | Rapid Review | Open Access Journal

Received November 11, 2019, accepted December 2, 2019, date of publication December 4, 2019,
date of current version December 19, 2019.

Digital Object Identifier 10.1109/ACCESS.2019.2957548

A Novel Methodology for Gain Enhancement of the Fabry-Pérot Antenna

PENG XIE, GUANGMING WANG, HAIPENG LI, (Student Member, IEEE), AND XIANGJUN GAO

Air and Missile Defense College, Air Force Engineering University, Xi'an 710051, China

Corresponding author: Guangming Wang (wgming01@sina.com)

This work was supported by the National Natural Foundation of China under Grant 61871394.

ABSTRACT A significant problem that is encountered with the traditional Fabry-Pérot cavity (FPC) antenna is the nonuniform phase distribution inside the cavity, which adversely affects the radiation characteristics of the antenna. In this paper, a novel methodology is proposed to further enhance the gain of the FPC antenna. A metasurface with a controllable reflection phase is designed to correct the phase distribution to a nearly uniform distribution, thereby enhancing the antenna gain. The unit cell of the metasurface is a simple substrate with two patches. The top layer patch is sufficiently large to provide high reflectivity, whereas the bottom layer patch has a variable size to tune the reflection phase of the unit cell. Using the proposed formula, a metasurface with a reflection phase correction is designed. The antenna gain is further enhanced, and high aperture efficiency is obtained. A prototype antenna is fabricated and measured. The measured results are in very good agreement with the simulated results. The measured results show that the antenna has a 3 dB gain bandwidth of 4% (9.8 GHz – 10.2 GHz). On average, a 2 dB gain enhancement is obtained Compare to the reference antenna. The maximum gain of the antenna reaches 19.7 dBi at 10 GHz with an aperture efficiency of 82.5%.

INDEX TERMS Fabry-Pérot antenna, metasurface, phase correction, gain enhancement, high efficiency, low profile.

I. INTRODUCTION

The Fabry-Pérot cavity (FPC) antenna exhibits high gain low profile characteristics and has thus attracted considerable attention since its initial introduction [1]. The FPC antenna has a simple structure that is easy to fabricate, results in the widespread used. Recent research on the FPC antenna has mainly focused on improving the bandwidth [2]–[9], realizing beam scanning [10], realizing circular polarization [11], [12], reducing the RCS [13] and enhancing the gain and efficiency [2], [14]–[21]. Among these objectives, enhancing the antenna gain is extremely important to significantly increase the aperture efficiency of the antenna.

Although the FPC antenna has high gain properties, the traditional antenna still exhibits defects that affect the gain. The most important problem is the nonuniform phase on the antenna aperture, and magnitude distribution also needs to be improved. Numerous methods exist to improve these defects to further enhance the antenna gain [2], [14]–[21]. One method is to compensate for the nonuniform phase on the antenna aperture plane [2], [14], [15]. A novel technique to design a dielectric phase correcting structure for an FPC antenna has been presented [14]. An all-dielectric phase correcting structure was designed to create a nearly uniform phase distribution on the antenna aperture plane. High gain and directivity and reduced side lobe levels are obtained by the proposed antenna. Second method is to correct the magnitude errors on the antenna aperture plane [16]–[18]. A single-layer nonuniform partially reflecting surface (PRS) has been presented to realize a high-gain and wideband [17]. This PRS has a nonuniform double-sided printed dielectric that exhibits a negative transverse-reflection magnitude gradient with a progressive reflection phase gradient over frequency. The proposed antenna realizes an improved bandwidth and peak directivity. Both phase and magnitude corrections are adopted to enhance the performance of the FPC antenna [19]. A systematic approach is proposed to correct the electric near-field phase and magnitude over a wide band for FPC antennas [19].

The associate editor coordinating the review of this manuscript and approving it for publication was Yang Yang.

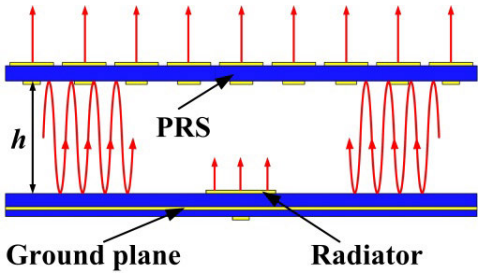

FIGURE 1. Schematic of FPC antenna.

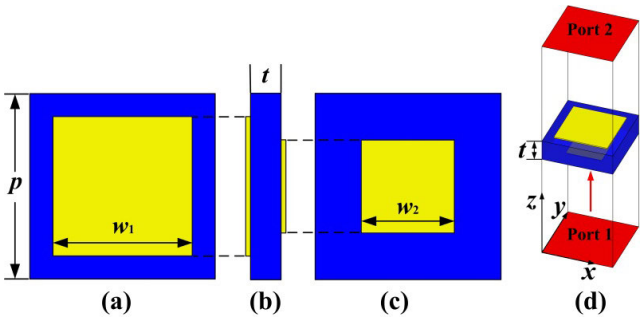

FIGURE 2. Geometry of unit cell. (a) top view; (b) side view; (c) bottom view; and (d) simulation model of unit cell.

A compact near-field correcting structure (NFCS), with a wide operational bandwidth, is designed to correct the near-field phase errors while applying a cosine-squared distribution to the near-field magnitude. Both gain enhancement and wideband properties are obtained. The use of a phase-correcting grating cover is also reported to enhance the gain of the beam scanning FPC antenna [20], [21].

The aforementioned reported methods to enhance the gain of the FPC antenna involve tuning either the phase of the near field of the aperture of the antenna or the transmission magnitude of the PRS. The nonuniform phase distribution on the antenna aperture plane is mainly caused by the nonuniform phase distribution in the internal cavity of the antenna. However, there are a few reports on the method that is based on tuning the reflection phase of the PRS to correct the nonuniform phase in the resonate cavity of the antenna. In this paper, a novel metasurface (MS) with reflection phase controllable properties is designed. The unit cell of the MS is a substrate with two patches. The top layer patch is sufficiently large to provide high reflectivity of the unit cell, whereas the bottom layer patch has a variable size to tune the reflection phase of the unit cell. An equation is proposed for the design of reflection phase of the MS to realize phase compensate of the FPC antenna. Thus the antenna gain is further enhanced and high aperture efficiency is obtained.

This paper is organized as follows. In Section II, the detailed properties of the unit cell are presented. The analysis and design of the MS and the FPC antenna are described in Section III. In Section IV, the simulation and measurement results are presented. Finally, conclusions are drawn in Section V.

II. UNIT CELL DESIGN

Fig. 1 is a schematic of the FPC antenna. The antenna consists of three components: a PRS, a ground plane and a radiator in the middle of the cavity formed by the PRS and the ground plane. The electromagnetic waves emanating from the radiator experience multiple reflections and transmissions in the cavity. On the basis of the theory presented in [22], the maximum directivity at the broadside is achieved when the equation (1) is satisfied, that is the waves exiting the cavity are in phase.

$$\varphi_S + \varphi_D - \frac{4\pi h}{\lambda_0} = 2N\pi, \quad N = 0, \pm 1, \pm 2 \ldots \tag{1}$$

In the equation above, λ_0 denotes the free space wavelength at the operating frequency, and φ_S and φ_D are the reflection phases of the PRS and the ground plane, respectively. Usually, the first resonance ($N = 0$) is adopted to maintain a low profile for the antenna. From Eq. (1), we can see that the parameters φ_S significantly affect the resonate state in the cavity. When the operating frequency is fixed, h varies with the reflection phase of the PRS (φ_S). Thus, a low antenna profile can be achieved by optimizing φ_S. Assuming that the size of the resonant cavity is infinite, the boresight directivity of the antenna relative to that of the feeding antenna can be calculated as [23]:

$$D_r = 10 \log \frac{1+R}{1-R} \tag{2}$$

where R denotes the reflection magnitude of the PRS. The equation above shows that, D_r is a function of R. The directivity can be increased to some extent by increasing R. Thus, a high reflectivity of PRS is necessary for a high gain FPC antenna. Experience shows that the maximum directivity is obtained when R is approximately 0.9 - 0.95. The antenna directivity is also related to the resonance state in the cavity. Below, we design a phase-gradient MS to improve the resonance state and enhance the gain of the FPC antenna.

The proposed phase-gradient MS is composed by the unit cell whose configuration is represented in Fig. 2. The unit cell has a size of 10×10 mm^2. It consists of two square patches located on the top and bottom sides of the substrate.

The substrate is F4B ($\varepsilon_{r,sub} = 2.65$, $\tan\delta = 0.0017$) with a thickness of 1.6 mm. Fig. 2 (a) is the top view of the unit cell, (b) is the side view, and (c) is the bottom view. The simulation model of the unit cell in the HFSS is shown in Fig. 2 (d). Master-slave boundaries are set along the x and y directions of the unit cell, and Floquet ports are set along the z direction. The incident plane wave propagates toward $+z$ direction in the simulation. The top patch is sufficiently large to provide a large reflectivity for the unit cell ($w_1 = 9$mm), and the bottom patch is used to control the reflection phase of the unit cell. Fig. 3 shows the simulation reflection coefficients of the unit cell when $w_2 = 4$ mm. We can see that, the reflection magnitude of the unit cell is approximately 0.95 at 10 GHz. Next, we simulate the reflection coefficients of the unit cell

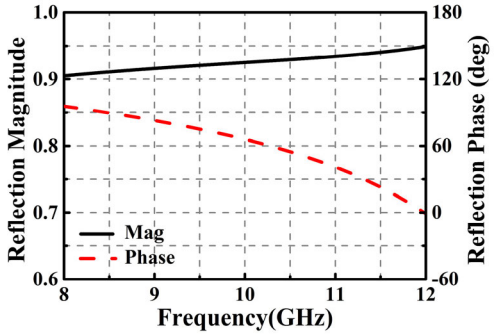

FIGURE 3. Simulated *S* parameters of unit cell with $w_2 = 4$mm.

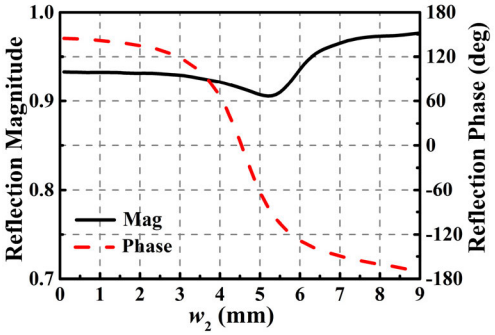

FIGURE 4. Effect of w_2 on *S* parameters of the unit cell at 10 GHz.

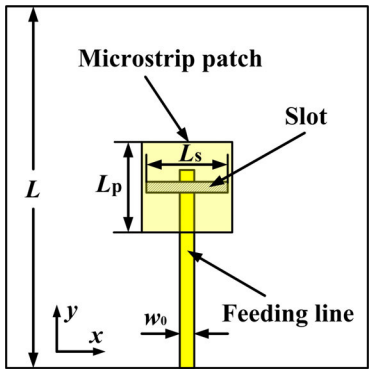

FIGURE 5. Sketch of feed antenna.

while varying w_2. The simulation results at 10 GHz are shown in Fig. 4. When w_2 is varied from 0 to 9, the reflection phase of the unit cell decreases from 150° to −170°, whereas the reflection magnitude of the unit cell is always larger than 0.9. This result shows that the proposed unit cell can realize reflection phase manipulation while maintaining a large reflectivity. Thus the MS formed by this unit cell exhibits a high reflectivity with the desired reflection phase distribution.

III. METASURFACE AND ANTENNA DESIGN

As an important part of the FPC antenna, the feed antenna should have a good performance. In this design, a slot coupled patch antenna, shown in Fig. 5, is chosen as the feeder for stable broadside radiation. This antenna consists of two

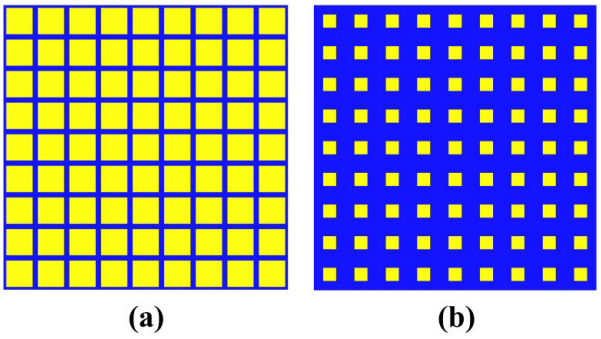

FIGURE 6. Configuration of MS1 (a) top view and (b) bottom view.

TABLE 1. Antenna parameters.

Parameters	Value (mm)	Parameters	Value (mm)
p	10	L	90
w_1	9	L_p	6.6
w_2	5	L_s	5.5
t	1.6	w_0	2.1

substrates with identical materials (F4B, $\varepsilon_{r,sub} = 2.65$, $\tan\delta = 0.0017$) but different thicknesses ($h_1 = 1.6$ mm and $h_2 = 0.8$ mm). A ground plane with a rectangular slot under the radiation patch is located between the two substrates. The radiation patch is printed on the top side of the upper substrate, and the feeding line is printed on the bottom side of the lower substrate. A 50 Ω SMA connecter is used to feed the antenna from the edge of the substrate. The dimensions of the feed antenna and the unit cell are shown in Table 1.

For a high gain antenna, a large size is preferred because to alleviate wave diffraction at the edge. However, considering the aperture efficiency, a compromise is adopted using the following method. The directivity of the proposed antenna is written as [23]:

$$D = D_f + D_r \tag{3}$$

where D_f is the directivity of the feed antenna (approximately 4.96 dBi), and D_r is about 15.48 dBi from equation (2) with $R = 0.945$. Thus, the directivity of the proposed antenna is approximately 20.4 dBi. Similar to a radiating aperture, the FPC antenna also has a Gaussian distribution with the magnitude of the electromagnetic field. Thus, to obtain the desired directivity, the antenna size can be estimated using the following equation [23], [24]:

$$A = \frac{10^{D/10} \times \lambda_0^2}{0.8\pi^2} \tag{4}$$

where A is the size of the square surface of the proposed antenna. An efficiency factor of 80%, which is deduced from a set of simulations, is used to modify the equation [24]. Considering the period of the unit cell and the objective of obtaining a high aperture, the size of the antenna is determined to be 3.6 $\lambda_0 \times$ 3.6 λ_0, which allows a directivity of

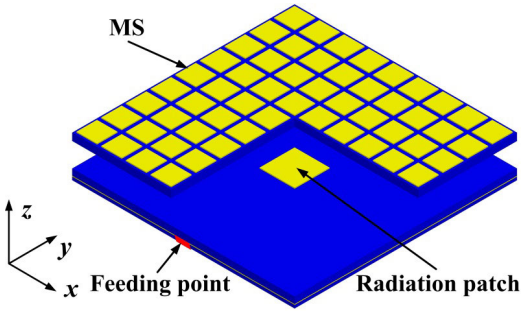

FIGURE 7. Geometry of proposed FPC antenna.

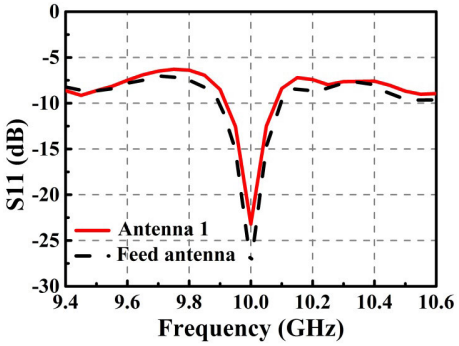

FIGURE 8. Simulation S11 of antenna 1.

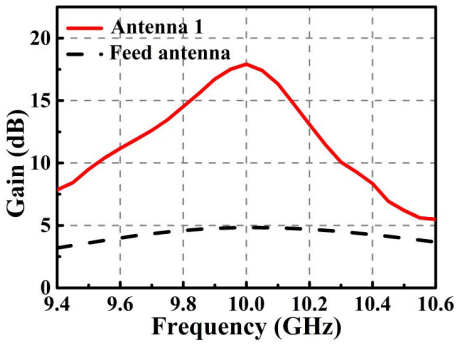

FIGURE 9. Simulation gain of antenna 1.

20.1 dBi. Consequently, the MS, with a dimension of 90 × 90 mm^2 and 9 × 9 units, as shown in Fig. 6, is used as the PRS to design the FPC antenna. The proposed MS is combined with the feed antenna to create the FPC antenna. The model of the proposed FPC antenna in HFSS is shown in Fig. 7.

First, we design an MS with a uniform phase distribution as a reference. MS1 consists of a unit cell with $w_1 = 9$ mm and $w_2 = 4$ mm. The top and bottom views of MS1 are shown in Fig. 6 (a) and (b), respectively. From Fig. 3, we find that a reflectivity of 0.94 and a reflection phase of 104° for MS1. The FPC antenna generated by MS1 and the feed antenna is named Antenna 1. Using the reflection phase of MS1 and Eq. (1), we obtain a height $h = 11.8$ mm for antenna 1. After optimization by HFSS, h is set to 12 mm. The simulated results of Antenna 1 are compared with those of the feed antenna in Figs. 8 and 9. Fig. 8 shows S11 for Antenna 1, and Fig. 9 shows the gain of Antenna 1. The S11 of Antenna 1 is similar to that of the feed antenna. This result shows that

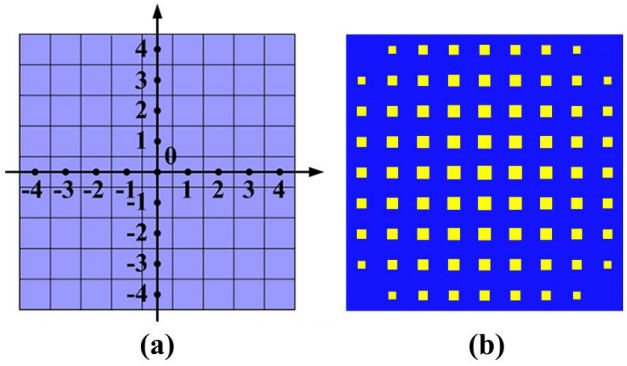

FIGURE 10. (a) Coding of unit cells and (b) bottom view of MS2.

incorporating the MS above the feed antenna does not affect the reflection coefficients of the antenna. Antenna 1 exhibits a large gain enhancement over that of the feed antenna. The maximum gain enhancement reaches 13 dB at 10 GHz.

To increase the gain of the FPC antenna further, MS2 is designed with a particular reflection phase distribution. Leading reflection phase at the edge and lagging reflection phase at the center are endowed to MS2. When a wave reflects off a surface, the reflected wave will tilt toward the region that has a lagging phase. Thus the lagging reflection phase at the center helps to concentrate the electromagnetic wave in the resonate cavity, thereby enhancing the antenna gain. We set the reflection phase to change linearly from the center to the edge. The reflection phase can be calculated using the following equation:

$$\varphi_{xy} = \varphi_0 + k\frac{\sqrt{x^2+y^2}\cdot p}{\lambda_0}\cdot 2\pi \quad x = -4,-3,-2,-1,0,1,2,3,4 \quad y = -4,-3,-2,-1,0,1,2,3,4 \tag{5}$$

where φ_{xy} denotes the reflection phase of the unit cell at (x, y), as shown in Fig. 10 (a); φ_0 denotes the reflection phase of the unit cell at the center (0,0) of MS2, and k is a phase compensation factor. The width of the bottom patch of the unit cell at (0, 0) is set at 5 mm, which fixes φ_0 at -63°. The reflection phases of the other unit cells are calculated using Eq. (5), and the sizes of the bottom patches of the other unit cells are obtained from Fig. 4, as shown in Fig. 10 (b). The antenna formed by the MS2 and the feed antenna is named Antenna 2. Except for the adopted MS, the other components of the two FPC antennas are identical.

Antenna 2 is also simulated by HFSS, and the phase compensation factor k is determined through simulations. Fig. 11 shows the simulated gain of Antenna 2 for different values of k and the gain of the Antenna 1. We can see that the FPC antenna with MS2 has a larger gain than the antenna with MS1. The highest gain performance of antenna 2 is obtained for $k = 0.03$. The gain enhancement by the Antenna 2 is on average 2 dB more than that by Antenna 1. To clearly determine the reason for the antenna gain enhancement, we observe the phase distribution of the antenna. Reference

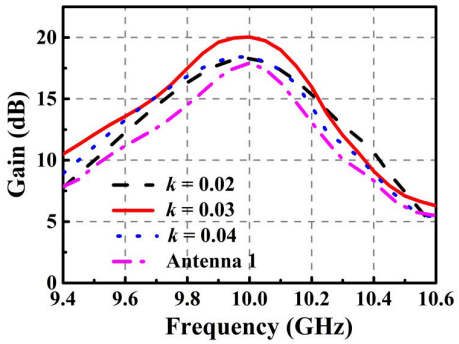

FIGURE 11. Simulation gain of antenna 2 for varying k.

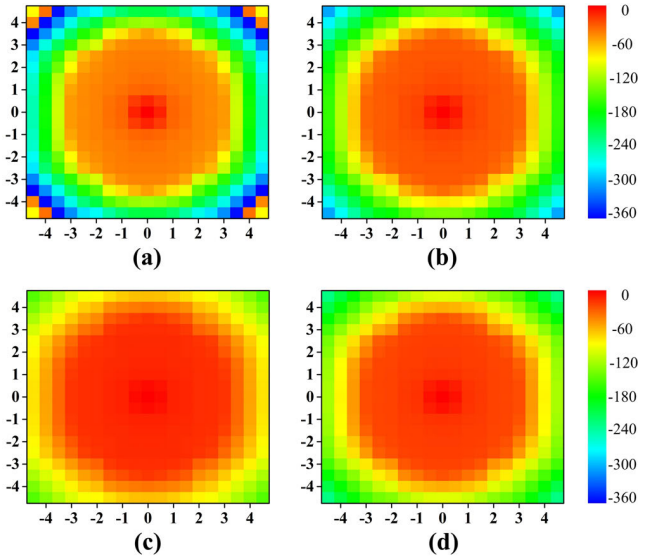

FIGURE 12. Phase distributions on reference plane 1: (a) antenna 1, (b) antenna 2 with $k = 0.02$, (c) antenna 2 with $k = 0.03$ and (d) antenna 2 with $k = 0.04$.

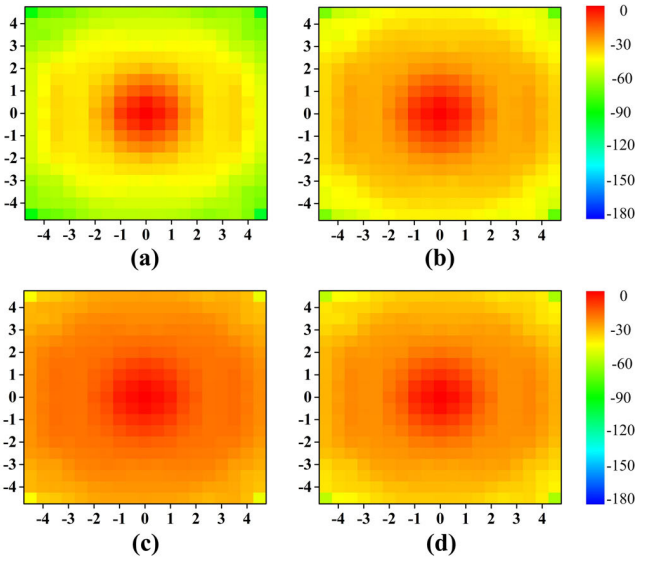

FIGURE 13. Phase distributions on reference plane 2: (a) antenna 1, (b) antenna 2 with $k = 0.02$, (c) antenna 2 with $k = 0.03$ and (d) antenna 2 with $k = 0.04$.

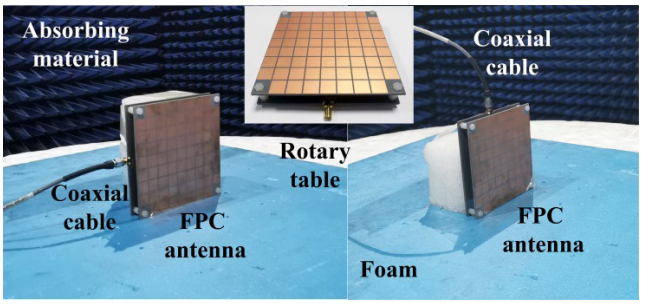

FIGURE 14. Fabricated antenna and measurement environment.

plane 1 is inside the cavity of the antenna, and plane 2 is outside the cavity. The distance between the reference planes to the MS are all 1 mm. The phase distribution at the reference plane 1 is shown in Fig. 12. We can see that Antenna 1 has a nonuniform phase distribution in the resonate cavity. Using MS2, the phase difference between center and edge of the cavity decreases. As a result, the antenna gain enhanced. When $k = 0.03$, the antenna has a nearly uniform phase distribution in the cavity and realize a highest gain. The simulator cannot distinguish between a forward traveling wave and a backward traveling wave. Thus, the phase distribution shown in Fig. 12 is the phase of the incident wave plus that of the reflected wave. Next, we plot the phase distribution for plane 2 in Fig. 13. The same trend shown in Fig. 12 for the phase variation is also seen in Fig. 13. That is, when $k = 0.03$, the antenna has a nearly uniform phase distribution both inside and outside the cavity. Thus, k is set to 0.03 to obtain the maximum gain enhancement, and the bottom view of the MS2 is shown in Fig. 10 (b). The S11 of antenna 2 for different values of k are similar to those for the feed antenna and are not shown for simplicity.

IV. SIMULATED AND MEASURED RESULTS

A prototype of antenna 2 is fabricated and measured. The unit cells at the four corners of the MS are removed and replaced by four holes, which are used to accommodate dielectric spacers to support the MS suspended on the feeding antenna. The simulation results show that this modification does not affect the performance of the antenna. Photographs of the fabricated FPC antenna and the measurement environment in the anechoic chamber are presented in Fig. 14. The reflection coefficients of antenna 2 are measured by the vector network analyzer. In Fig. 15, the simulated and measured S11 are plotted for antenna 2 and the feed antenna. The S11 of antenna 2 is similar to that of the feed antenna, and the measured results agree well with the simulated results. The simulated -10 dB bandwidth of the antenna is 9.92 – 10.08 GHz and the measured -10 dB bandwidth is 9.91 – 10.1 GHz. The simulated and measured realized gains of antenna 2 are shown in Fig. 16. Good agreement is obtained between the simulated

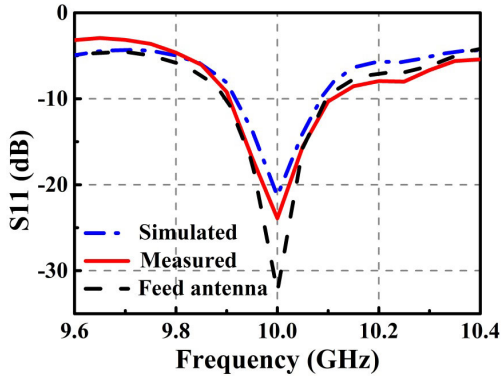

FIGURE 15. Simulated and measured S11 of proposed antenna.

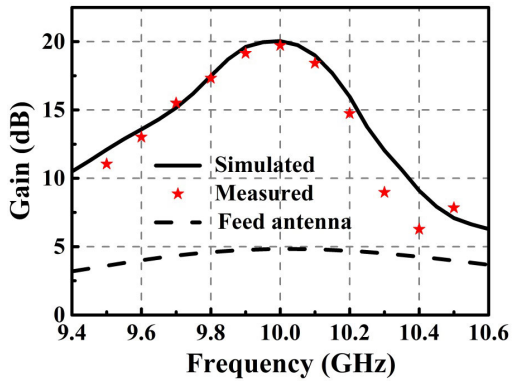

FIGURE 16. Simulated and measured realized gain for proposed antenna.

TABLE 2. Comparison of the proposed antenna with previously reported antennas.

Ref.	Frequency (GHz)	Method	Max gain (dBi)	Profile (λ_0)	Efficiency
[14]	10 - 17.6	Near field phase correction	10.2	0.9	86%
[15]	10.9-12.5	Near field phase correction	20.6	2.4	33%
[16]	10-12	Near field phase correction	21	1.8	35%
[17]	5.71 - 5.98	Magnitude tuning	20.4	1	91%
[18]	10.1-14.9	Near field phase correction	15.75	0.7	78%
[19]	9.66-15.47	Magnitude tuning	20.6	2.3	70%
proposed	9.92-10.08	Internal phase correction of cavity	19.7	0.53	82.5%

and measured results. The measured maximum gain of the antenna is 19.7 dBi at 10 GHz, which is 0.3 dBi less than the simulated result. The aperture efficiency of the proposed antenna is calculated to be 82.5%. Antenna 2 achieves a maximun gain enhancement of 14.9 dB over that of the feed antenna. The measured 3 dB gain bandwidth of the antenna is 9.76 – 10.14 GHz, which is larger than the impedance bandwidth.

Another important performance of the antenna is the radiation patterns. The radiation patterns of antenna 2 are measured in an anechoic chamber. The simulated and measured radiation patterns in the *xoz* and *yoz* planes at 10 GHz are plotted in Fig. 17. The antenna exhibits good radiation characteristics, with a side lobe level less than −12 dB and a cross-polarization level less than −23 dB. The measured main lobe of antenna 2 in the *yoz* plane agrees well with the simulated results and the measured main lobe in the *xoz* plane is a little wider than the simulated result.

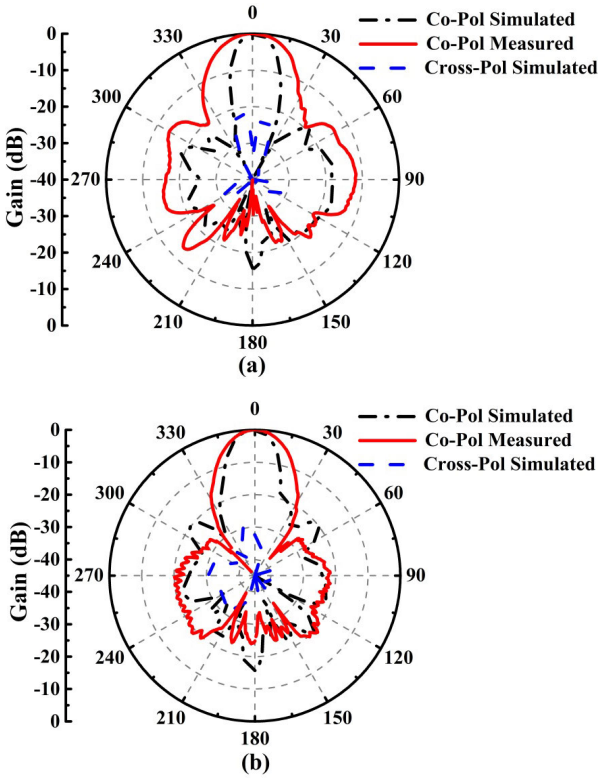

FIGURE 17. Radiation patterns of antenna: (a) *xoz* plane; (b) *yoz* plane.

Table 2 is a comparison of the proposed antenna with previously reported antennas. The antenna that is designed with the proposed method can realize a high gain and high aperture efficiency with a very low profile.

V. CONCLUSION

A reflection phase controllable unit cell is proposed in this paper. An MS based on this unit cell with a uniform reflection phase is used to form a high gain FPC antenna with a slot coupled patch antenna. To further enhance the gain of the FPC antenna, a novel methodology is proposed to design an MS with leading reflection phase at the edge and lagging reflection phase at the center. The designed reflection phase distribution increases the gain of the FPC antenna. A prototype antenna is fabricated and measured. The maximum gain of the FPC antenna reaches 19.7 dBi, which is 2 dBi higher than the reference antenna and 14.9 dB higher than the feed antenna. The proposed antenna also exhibits good radiation pattern performance. The proposed method can also be applied for the gain enhancement of other FPC antennas.

REFERENCES

[1] F. Qin, S. Gao, Q. Luo, G. Wei, J. Xu, J. Li, C. Wu, C. Gu, and C. Mao, "A triband low-profile high-gain planar antenna using Fabry–Pérot cavity," *IEEE Trans. Antennas Propag.*, vol. 65, no. 5, pp. 2683–2688, May 2017.
[2] A. A. Baba, R. M. Hashmi, and K. P. Esselle, "Achieving a large gain-bandwidth product from a compact antenna," *IEEE Trans. Antennas Propag.*, vol. 65, no. 7, pp. 3437–3446, Jul. 2017.
[3] Y. Zheng, J. Gao, Y. Zhou, X. Cao, H. Yang, S. Li, and T. Li, "Wideband gain enhancement and RCS reduction of Fabry–Pérot resonator antenna with chessboard arranged metamaterial superstrate," *IEEE Trans. Antennas Propag.*, vol. 66, no. 2, pp. 590–599, Feb. 2018.
[4] S. Zarbakhsh, M. Akbari, F. Samadi, and A.-R. Sebak, "Broadband and high-gain circularly-polarized antenna With low RCS," *IEEE Trans. Antennas Propag.*, vol. 67, no. 1, pp. 16–23, Jan. 2019.
[5] R. Lian, Z. Tang, and Y. Yin, "Design of a broadband polarization-reconfigurable Fabry–Pérot resonator antenna," *IEEE Antennas Wireless Propag. Lett.*, vol. 17, no. 1, pp. 122–125, Jan. 2018.
[6] M. L. Abdelghani, H. Attia, and T. A. Denidni, "Dual- and wideband Fabry–Pérot resonator antenna for WLAN applications," *IEEE Antennas Wireless Propag. Lett.*, vol. 16, pp. 473–476, 2017.
[7] Q.-Y. Guo and H. Wong, "Wideband and high-gain Fabry–Pérot cavity antenna with switched beams for millimeter-wave applications," *IEEE Trans. Antennas Propag.*, vol. 67, no. 7, pp. 4339–4347, Jul. 2019.
[8] H. Attia, M. L. Abdelghani, and T. A. Denidni, "Wideband and high-gain millimeter-wave antenna based on FSS Fabry–Pérot cavity," *IEEE Trans. Antennas Propag.*, vol. 65, no. 10, pp. 5589–5594, Oct. 2017.
[9] N. Wang, L. Talbi, Q. Zeng, and J. Xu, "Wideband Fabry–Pérot resonator antenna with electrically thin dielectric superstrates," *IEEE Accesss*, vol. 6, pp. 14966–14973, 2018.
[10] B. Ratni, A. de Lustrac, G.-P. Piau, and S. N. Burokur, "Modeling and design of metasurfaces for beam scanning," *Appl. Phys. A, Solids Surf.*, vol. 123, no. 50, pp. 5589–5594, Dec. 2016.
[11] L. Zhang and T. Dong, "Low RCS and high-gain CP microstrip antenna using SA-MS," *Electron. Lett.*, vol. 53, no. 6, pp. 375–376, Mar. 2017.
[12] C. Chen, Z.-G. Liu, H. Wang, and Y. Guo, "Metamaterial-inspired self-polarizing dual-band dual-orthogonal circularly polarized Fabry–Pérot resonator antennas," *IEEE Trans. Antennas Propag.*, vol. 67, no. 2, pp. 1329–1334, Feb. 2019.
[13] L. Zhang, X. Wan, S. Liu, J. Y. Yin, Q. Zhang, H. T. Wu, and T. J. Cui, "Realization of low scattering for a high-gain Fabry-Pérot antenna using coding metasurface," *IEEE Trans. Antennas Propag.*, vol. 65, no. 7, pp. 3374–3383, Jul. 2017.
[14] M. U. Afzal, K. P. Esselle, and B. A. Zeb, "Dielectric phase-correcting structures for electromagnetic band gap resonator antennas," *IEEE Trans. Antennas Propag.*, vol. 63, no. 8, pp. 3390–3399, Aug. 2015.
[15] M. U. Afzal, K. P. Esselle, and A. Lalbakhsh, "A methodology to design a low-profile composite-dielectric phase-correcting structure," *IEEE Antennas Wireless Propag. Lett.*, vol. 17, no. 7, pp. 1223–1227, Jul. 2018.
[16] L. Zhou, X. Chen, and X. Duan, "Fabry–Pérot resonator antenna with high aperture efficiency using a double-layer nonuniform superstrate," *IEEE Trans. Antennas Propag.*, vol. 66, no. 4, pp. 2061–2066, Aug. 2018.
[17] A. Lalbakhsh, M. U. Afzal, K. P. Esselle, S. L. Smith, and B. A. Zeb, "Single-dielectric wideband partially reflecting surface with variable reflection components for realization of a compact high-gain resonant cavity antenna," *IEEE Trans Antennas Propag.*, vol. 67, no. 3, pp. 1916–1921, Mar. 2019.
[18] A. K. Singh, M. P. Abegaonkar, and S. K. Koul, "High-gain and high-aperture-efficiency cavity resonator antenna using metamaterial superstrate," *IEEE Antennas Wireless Propag. Lett.*, vol. 16, pp. 2388–2391, 2017.
[19] A. Lalbakhsh, M. U. Afzal, K. P. Esselle, and S. L. Smith, "Wideband near-field correction of a Fabry–Pérot resonator antenna," *IEEE Trans. Antennas Propag.*, vol. 67, no. 3, pp. 1975–1980, Mar. 2019.
[20] W. Ma, W. Cao, S. Shi, Z. Zeng, and X. Yang, "Gain enhancement for circularly polarized SIW frequency beam scanning antenna using a phase-correcting grating cover," *IEEE Access*, vol. 7, pp. 52680–52688, 2019.
[21] W. Cao, W. Hong, Z. N. Chen, B. Zhang, and A. Liu, "Gain enhancement of beam scanning substrate integrated waveguide slot array antennas using a phase-correcting grating cover," *IEEE Trans. Antennas Propag.*, vol. 62, no. 9, pp. 4584–4591, Sep. 2014.
[22] G. Von Trentini, "Partially reflecting sheet arrays," *IRE Trans. Antennas Propag.*, vol. 4, no. 4, pp. 666–671, Oct. 1956.
[23] N. Wang, Q. Liu, C. Wu, L. Talbi, Q. Zeng, and J. Xu, "Wideband Fabry–Pérot resonator antenna with two complementary FSS layers," *IEEE Trans. Antennas Propag.*, vol. 62, no. 5, pp. 2463–2471, May 2014.
[24] L. Leger, C. Serier, R. Chantalat, M. Thevenot, T. Monediere, and B. Jecko, "1-D dielectric EBG resonator antenna design," *Annal. Télé-Commun.*, vol. 59, nos. 3–4, pp. 242–260, 2004.

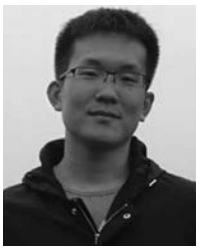

PENG XIE was born in Henan, China. He received the bachelor's and master's degrees from Air Force Engineering University (AFEU), Xi'an, China, in 2015 and 2017, respectively, where he is currently pursuing the Ph.D. degree in electrical science and technology. His research interests include metamaterials and antenna design.

GUANGMING WANG was born in China, in 1964. He received the B.S. and M.S. degrees in electromagnetic field and microwave technology from Air Force Engineering University, Xi'an, China, in 1982 and 1990, respectively, and the Ph.D. degree in electromagnetic field and microwave technology from the University of Electronic Science and Technology, Chengdu, China, in 1994.

He joined Air Force Engineering University, as an Associate Professor, and was promoted to Full Professor, in 2000, where he is currently the Head of the Microwave Laboratory. He has authored or coauthored more than 100 conference and journal articles. His current research interests include microwave circuits, antennas, and also the new structures, including EBG, PBG, metamaterials, and fractals. He has been a Senior Member of the Chinese Commission of Communication and Electronic. Since 1994, he has been awarded and warranted several items supported under the National Natural Science Foundation of China and fulfilled many local scientific research programs.

HAIPENG LI (S'16) was born in China, in 1991. He received the B.S. and M.S. degrees in electromagnetic field and microwave technology from Air Force Engineering University, Xi'an, China, in 2013 and 2015, respectively, where he is currently pursuing the Ph.D. degree.

His research interests include metamaterials, metasurfaces, and their applications to novel antennas and multifunctional devices. He has published more than ten peer-reviewed first-author articles in the IEEE TRANSACTION ON ANTENNAS AND PROPAGATION, IEEE ANTENNAS AND WIRELESS PROPAGATION LETTERS, and *Progress in Electromagnetics Research*.

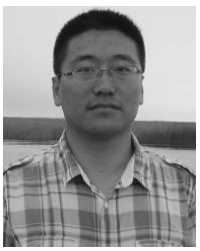

XIANGJUN GAO was born in Shanxi, China, in 1979. He received the B.S., M.S., and Ph.D. degrees in electromagnetic field and microwave technology from Air Force Engineering University, Xi'an, China, in 2001, 2004, and 2008, respectively.

He is currently an Assistant Professor with Air Force Engineering University. His research interests include microwave circuits, antennas, and arrays.